

A preliminary investigation into determining CC0 π cross-section sensitivities in SBND and performing a GENIE global fit to neutrino scattering data



Rhiannon Jones
University of Liverpool
School of Physical Sciences
rjones@hep.ph.liv.ac.uk

1st year PhD report

Abstract

Random stuff

1. Introduction

Neutrino physics is at the core of current high energy research. One of the profound discoveries made in recent years was the observation of neutrino flavour oscillations by the Super-Kamiokande (Super-K) experiment, which was the first confirmation that physics existed beyond the standard model of particle physics. In brief, neutrinos described by the standard model would be massless particles, but since the flavours are made up of superpositions of mass states, the oscillation of the flavour states implies that the relative mass states are different, and therefore non-zero [1].

Future, long-baseline, neutrino experiments such as the Deep Underground Neutrino Experiment (DUNE) and Hyper-Kamiokande (Hyper-K) are hoping to investigate some of the most fundamental questions we are still asking: Why does the universe consist of matter, and not anti-matter? What is the neutrino mass hierarchy? Neutrino research is an extremely active field. Optimising the current and future detectors to maximise the accuracy of all interaction analyses is a crucial step towards obtaining concrete answers to these questions.

A brief introduction to the topics covered in this report is as follows, more detail on each will be given in later sections.

1.1. *Neutrino interactions*

Due to the elusive nature of the neutrino, directly observing one in a detector isn't possible. It is therefore necessary to infer their existence from particles produced when they interact. Since this process relies upon the reconstruction capability of the experiment, purpose-built detectors will attempt to maximise the efficiency of this.

Another property of the neutrino which poses a significant difficulty within detectors is their interaction probability, or cross-section. A typical neutrino cross-section is on the order of 10^{-44} cm^2 which corresponds to ~ 1 interaction every 10 light years in steel, for neutrinos with only a few MeV energy [2]. This fact introduces the need for the interacting neutrinos to have high energies in these dedicated experiments, if we are to sufficiently reduce their mean free path. More detail on this topic will be discussed in section 3.

1.2. *GENIE and the GENIE-Professor global fits*

GENIE is the world leading Monte Carlo neutrino interaction generator. Generators are a crucial machinery in all high energy physics analyses as they use theoretical models to produce predictions of how and where neutrino interactions will occur in specific detector geometries [3]. With this information, comparisons between experimental data and theoretical predictions can be drawn, the models can be improved through fits to such data and potential new physics can be explored. These predictions also help motivate the requirements for building state-of-the art detectors and produce high precision cross-section measurements to improve current and future neutrino physics analyses.

An effort to improve model configurations by performing fits to an archive of experimental data is currently being carried out by GENIE using the Professor software frame-

work, which was written with this purpose for experiments at the LHC [4]. The ultimate goal of this exercise is to perform a global fit to all neutrino scattering data and consequently produce comprehensive model configurations to further optimise the predictions made for the next generation of neutrino experiments. This work and GENIE's role in current and future neutrino experiments will be discussed further in section 5.

1.3. Cross-sections

In order to correctly model neutrino events within a specific detector geometry and material, certain parameters have to be known. In particular, the probability of an interaction taking place - its cross-section - is required for each possible interaction the neutrino could undergo. Cross-section measurements are therefore a necessity for the Monte Carlo event generators, and consequently the future detector studies mentioned earlier.

The extent of our current knowledge of charged current neutrino cross sections is shown in Figure 1. The plot contains cross-section information from multiple types of neutrino experiment, differing in both target material and detector machinery. A feature of this plot which is of the most interest to a Short Baseline Near Detector (SBND) cross-section study in particular, is the lack of precision in the measurements made towards the ~ 1 GeV region [5]. SBND will not only be operational at this energy range, but it will also have statistics substantial enough to potentially make a significant contribution to improving the current knowledge in this region.

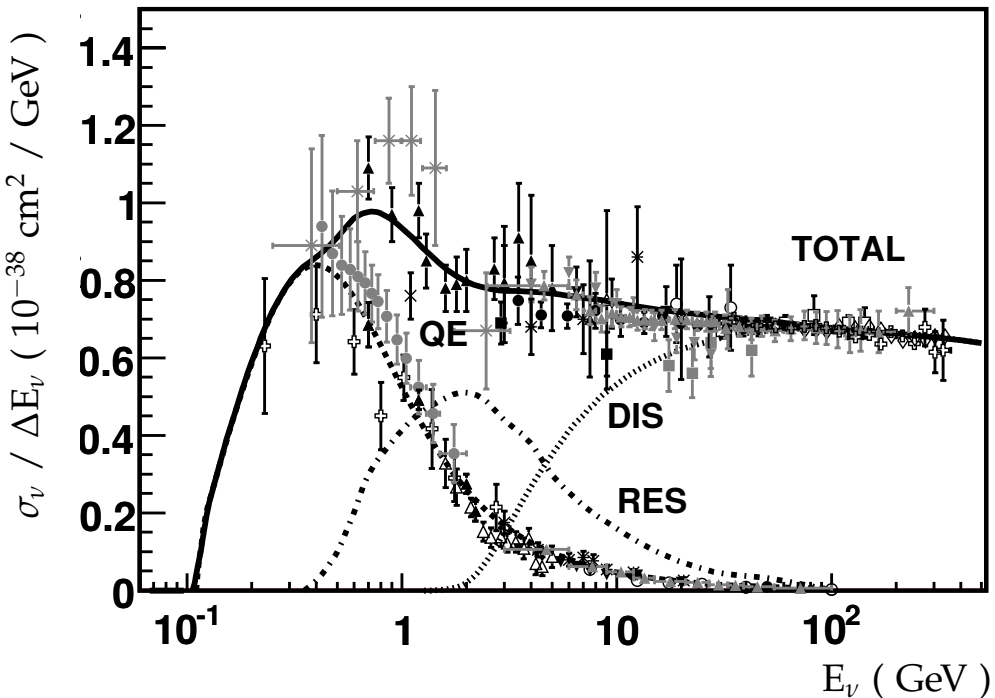


Figure 1: A compilation of the total cross-section data across the ~ 1 MeV to ~ 100 GeV energy range. Including a breakdown in terms of the quasi-elastic, QE, resonant, RES and deep inelastic scattering, DIS, topologies [5].

The scale of contribution SBND could make to this area of physics would in turn

improve the predictions made by event generators for the next generation of neutrino experiments. Cross-sections will be discussed further in section 6.

1.4. SBND Physics Goals

SBND is one of 3 liquid argon detectors using the same neutrino beam in the Short Baseline Neutrino (SBN) program. Together, they aim to explore neutrino oscillations at 3 different positions along the beam, allowing for highly sensitive measurements to be made [6].

Another objective of the SBN program, along with many other neutrino physics experiments, is to observe or reject the existence of sterile neutrinos. Though this will not be discussed here.

The MiniBooNE and LSND experiments observed an excess of low energy electron neutrino appearance in their data [7]. One of the main physics goals of SBND is to look for and characterise this excess, in collaboration with any results obtained by the MicroBooNE experiment before SBND is taking data. The beamline of MicroBooNE is 470m compared to 110m for SBND, whether one or both experiments observe the excess will tell us if there was a dependence on the distance travelled by the neutrinos [6].

This report will further describe the current status of neutrino cross-section analyses, the level importance that these measurements have in the field, and how a sensitivity calculation in the low GeV energy region is being carried out. It will then explain in more detail how Monte Carlo neutrino generators can be, and are being improved using recent and historical scattering data, through a global fit of comprehensive theoretical model configurations.

2. Detector functionality and features of the experiment

2.1. Booster neutrino beam, BNB

A Booster Neutrino Beam (BNB) of muon neutrinos is formed by firing protons, taken from an accelerator with ~ 8 GeV kinetic energy, at a beryllium target which produces a hadronic beam consisting mainly of pions. The pions in this beam are then focussed and polarised before they decay, mostly to muon neutrinos, which propagate into the TPC where they interact with the target material. The beam's high muon neutrino excess occurs because the dominant decay channel of pions is (1) [6],

$$\pi^+ \longrightarrow \mu^+ + \nu_\mu \quad (1)$$

and the branching ratio of pions decaying to electrons over muons on the order of $\sim 10^{-4}$ due to the relation given in equation (2) [8].

$$R_\pi = \left(\frac{m_e}{m_\mu} \right)^2 \left(\frac{m_\pi^2 - m_e^2}{m_\pi^2 - m_\mu^2} \right)^2 \sim 10^{-4} \quad (2)$$

The beam fires neutrinos directly into the time projection chamber (TPC) of an experiment at such velocities that it can always be assumed that the particles entered the TPC from one direction and, before interacting, were forward-going. This technicality gives an immediate criteria for the removal of backgrounds, such as cosmogenic neutrinos, which would enter the TPC from all directions [6].

2.2. Liquid argon time projection chambers, LArTPC

In current and future neutrino experiments such as DUNE and the short baseline neutrino (SBN) program (SBND, MicroBooNE and ICARUS), liquid argon is the target material of the detector. Argon in this form is used due to its stability and purity as a noble gas, its high density and its low cost. These properties lead to resolution capabilities on the order of the Bubble Chamber experiments, which allows for high certainty in distinguishing between interactions and ultimately optimises the resolving power of the experiment [9]. An example event display in liquid argon from the MicroBooNE experiment is given in Figure 2 [10].

Once the neutrino has entered the TPC it interacts with an argon atom to produce final state particles in the detector. These particles may then decay, be absorbed or interact with the argon in the TPC. Ionization electrons and photons are also produced through these interactions.

A general purpose LArTPC diagram is given in Figure 3. A brief description of its functionality is as follows [11]:

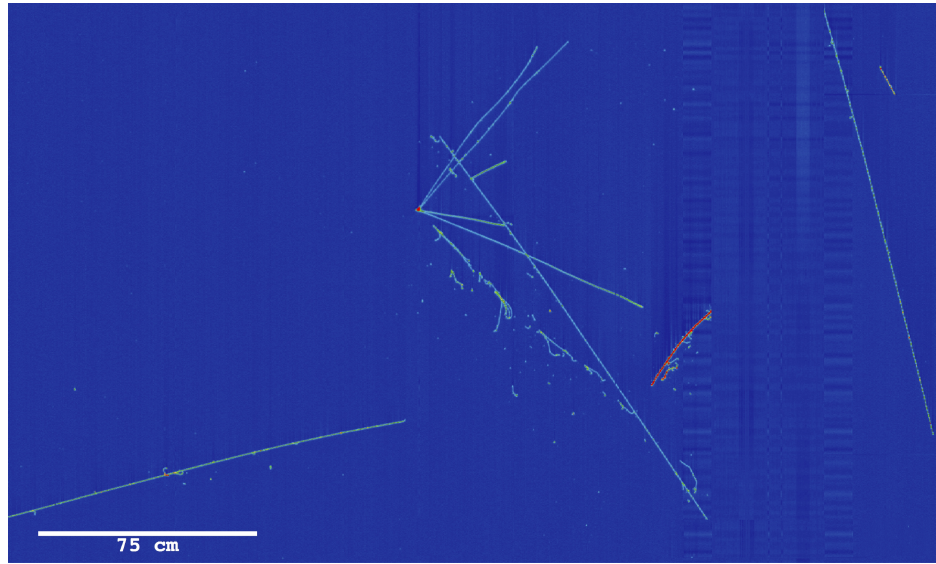


Figure 2: An example event display from the MicroBooNE detector, one of the first to be seen in a liquid argon TPC. The resolving power is high enough for the tracks and showers to be clearly distinguished, along with the interaction vertex of the event [10].

- A potential difference is induced between the cathode and anode planes
 - Electric field is induced by the potential difference
 - Ionization electrons are caused to drift towards the three planes of wires on the opposite, anode side of the TPC
- Electron hits on the wires are converted to a current read out
 - Timing and spatial information deduced about the event
- Induction wire planes, U & V are situated at 60° to the vertical collection plane, Y
 - Full 3 dimensional read out is possible
 - Spatial information gives the y & z co-ordinates
 - Timing information determines the x co-ordinate
- Photons cascade into showers and reach the wall of PMTs residing behind the wire planes
 - Prompt scintillation light hits the PMTs
 - Provides additional information about the x co-ordinate of the event

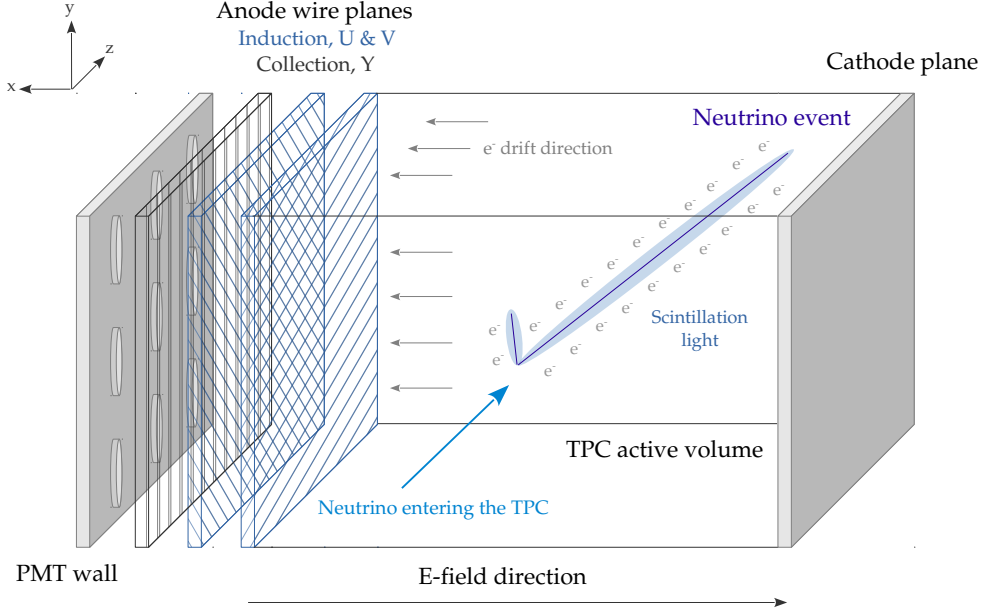


Figure 3: An example neutrino interaction within a typical LArTPC. The ionization electrons drift in what is defined as the positive x -direction as shown, and the scintillation light would be collected by the wall of PMTs behind the wire planes. The induction planes U and V are at 60° to the vertical collection plane Y . The neutrino would enter the TPC in the positive z -direction.

2.3. SBND

SBND will have a beamline of 110m, the shortest in the SBN program. At this distance, the flux of the neutrino beam is ~ 100 times that of the other 2 SBN detectors, these relative fluxes are simulated as a function of neutrino energy and shown graphically in Figure 4 [6]. Consequently, the number of events expected during the full exposure of the experiment is around 7,000,000. A breakdown in terms of individual processes is given in Figure 5 [6]. Combining these huge statistics with the exceptional resolution capabilities of the liquid argon TPCs will allow SBND to make unprecedentedly high-precision cross-section and oscillation measurements. Working both in conjunction with MicroBooNE and ICARUS, and as a stand-alone experiment, SBND should produce some exciting and extremely important results.

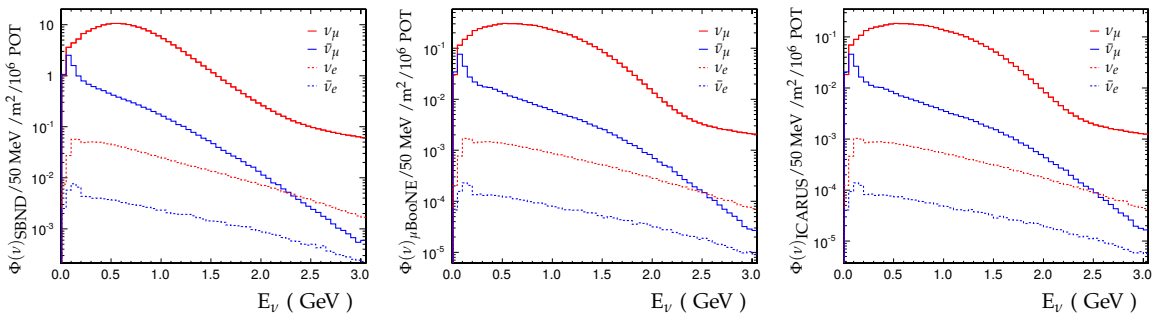


Figure 4: From left to right, the BNB fluxes of SBND, MicroBooNE (μ BooNE and ICARUS. From these plots it can be seen that SBND's flux will be ~ 100 times the other two [6].

Process		No. Events
ν_μ Events		
CC 0 π	$\nu_\mu N \rightarrow \mu + Np$	3,551,830
CC 1 π^\pm	$\nu_\mu N \rightarrow \mu + nucleons + 1\pi^\pm$	1,161,610
CC $\geq 2\pi^\pm$	$\nu_\mu N \rightarrow \mu + nucleons + \geq 2\pi^\pm$	97,929
CC $\geq 1\pi^0$	$\nu_\mu N \rightarrow \mu + nucleons + \geq 1\pi^0$	497,963
<hr/>		
NC 0 π	$\nu_\mu N \rightarrow nucleons$	1,371,070
NC 1 π^\pm	$\nu_\mu N \rightarrow nucleons + 1\pi^\pm$	260,924
NC $\geq 2\pi^\pm$	$\nu_\mu N \rightarrow nucleons + \geq 2\pi^\pm$	31,940
NC $\geq 1\pi^0$	$\nu_\mu N \rightarrow nucleons + \geq 1\pi^0$	358,443
<hr/>		
Total ν_μ & ν_e events		7,251,948

Figure 5: Some expected statistics for the entire exposure of SBND, broken down into some of the processes by which the neutrino may interact [6].

SBND will be 5m long, 4m tall and 4m wide holding a total of 112 tonnes of liquid argon in its active volume. As an LArTPC, SBND will function in mostly the same way as described earlier and in Figure 3, although it will have some unique features. Figure 6 gives an idea of how the detector will be constructed.

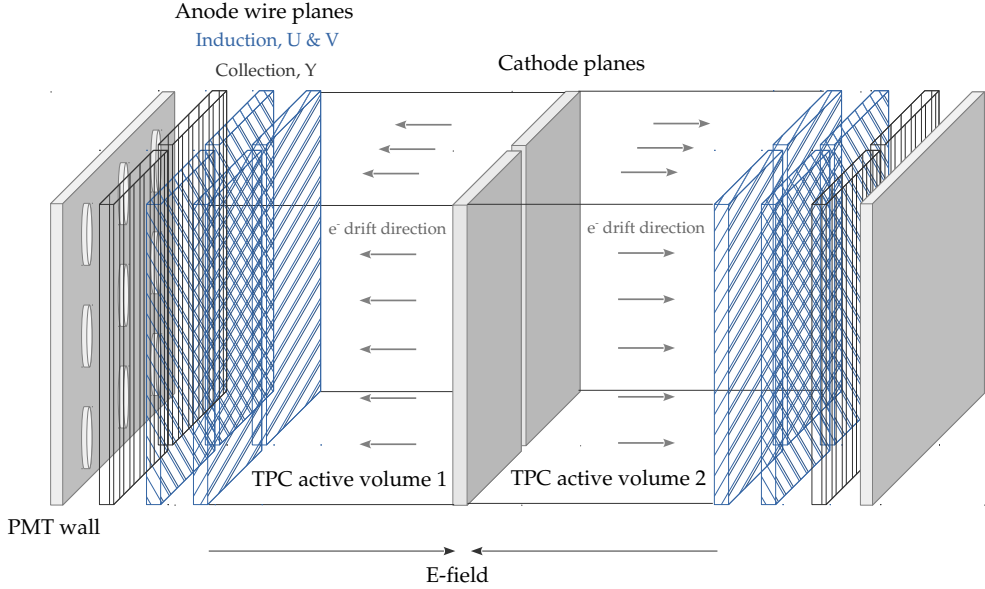


Figure 6: A diagram to give an idea of how the SBND detector will look. It features many similarities to the standard liquid argon TPC design, but applies the concept of multiple modules - this is a possibility for the structure of DUNE [6].

Unlike the typical TPC setup, SBND will have 2 cathode planes, 4 anode planes and 2 time projection chambers. The cathode planes will lie side-by-side, positioned at the join between the two TPCs. The anode planes will also lie in twos next to one another, with a pair residing on the opposite wall to the cathode plane of each TPC. This allows for 2 electric fields and therefore 2 opposing drift directions. In the same way as shown in Figure 3, there will be 3 wire planes to each anode plane. In the gaps between two adjacent anode planes, electrodes will divert the approaching particles towards the nearest active parts of the plane [6]. The multiple module system may well be a feature of the next generation TPC detectors such as DUNE.

3. Neutrino Interaction Phenomenology in the few-GeV Energy Range

3.1. Dominant topologies

The statistics given in Figure 5 indicate that the dominant interactions observable in SBND will be CC0 π and CC1 π^\pm , example Feynman diagrams of the main contributing processes at the free-nucleon level are given in Figure 7.

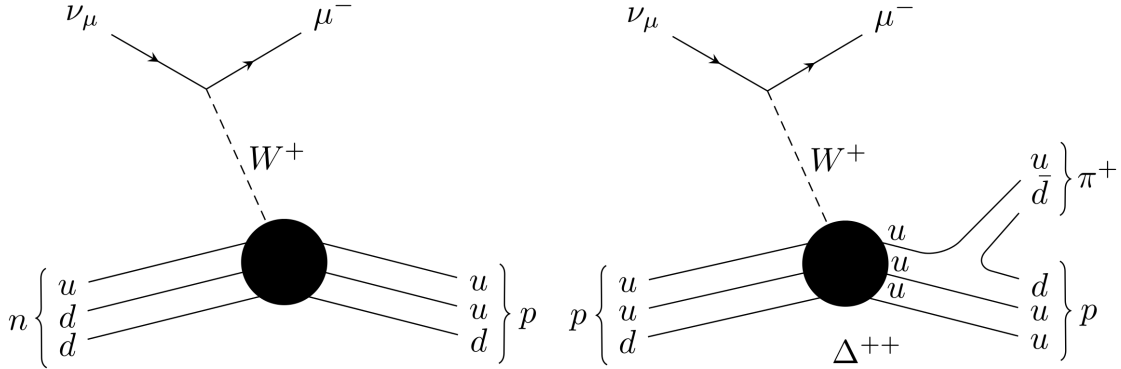


Figure 7: On the left-hand side is a Feynman diagram of the CCQE interaction. During this process, the incoming neutrino interacts with a neutron and produces a muon and a single proton as the observable final state particles. On the right is the positive version of the CC1 π^\pm interaction, in which a neutrino interacts with a proton emitting a π^+ alongside the final state muon and proton. Here, the invariant mass of the entire hadronic system must be accounted for when reconstructing the neutrino energy.

One dominant background to the CC0 π process is an NC1 π^\pm interaction, in which the final state pion may decay rapidly into a muon leaving the appearance of a single proton and muon final state as described in equations (4).

$$p + \nu_\mu \longrightarrow \nu_\mu + p + \pi^- \quad (3)$$

$$\downarrow \quad (4)$$

$$\pi^- \longrightarrow \mu^- + \bar{\nu}_\mu \quad (5)$$

Backgrounds such as this are an important consideration in all analyses. Though in high resolution detectors such as SBND, the ability to distinguish true signal should be possible to the extent that impurity contributions are minimal.

3.2. Energy reconstruction

The energy of the incoming neutrino must be reconstructed from the other particles involved in the interaction. When dealing simply with a 2-body hadronic process, such as the one shown in the left hand side of Figure 7, it is acceptable to use the quasi-elastic estimation (6) [12] to calculate the reconstructed energy, \bar{E}_ν . Where E_μ , m_μ and k'_μ are the energy, mass and 3-momentum of the final state muon, M_N is the mass of a target nucleon and θ is the opening angle between the outgoing muon and proton [12].

$$\bar{E}_\nu = \frac{E_\mu - m_\mu^2/(2M_N)}{1 - (E_\mu - |\underline{k}'_\mu| \cos\theta)/M_N} \quad (6)$$

Alternatively, if the interaction involves more particles in the final state, such as multiple protons or pions escaping the nucleus, one must account for the energy given to all of the hadronic final state particles in the energy reconstruction.

3.3. Complications in the free nucleon theory

Theoretical models of physical interactions on free nucleons are well-grounded, since any incoming particles will interact entirely externally to the particles they collide with. However, when dealing with nuclear targets in high energy physics experiments, such as SBND, complications occur in our understanding of the true nature of the interactions taken place, and data can become inexplicable in comparison with models built on free nucleon cross sections [14].

For instance, in the few-GeV energy range, neutrinos will be able to penetrate the argon nucleus and interact with individual nucleons. Therefore, an observation of the CC0 π interaction in SBND would not necessarily indicate that a CCQE process took place between the neutrino and nucleon. Pions may be produced initially but be absorbed before ever escaping, thus leaving them invisible to the detector, this is visualised in Figure 8.

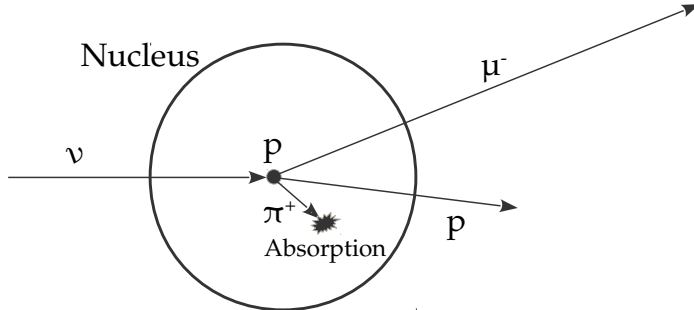


Figure 8: A schematic of a potential interaction which may occur within the nucleus of an argon atom in SBND, leaving the pion invisible to the detector and the true interaction unidentifiable.

Another phenomenon that is not accounted for in the free nucleon theory is the potential for multiple nucleons to be involved in the initial scattering process. Such nucleons proceed to leave the nucleus and can appear to be products of an unphysical interaction such as the one in equation (7),



when in fact, the interaction in equation (8),



actually occurred within the nucleus, which is known as the 2-particle 2-hole effect, dominated by the Meson Exchange Current (MEC) [13].

In recent experiments, an excess of scattering events have been observed with respect to the theoretical predictions. It is now believed that MEC could be responsible, and it is therefore a primary concern of theorists, neutrino event generators and nuclear physicists to work together in correctly simulating what may occur in all future neutrino experiments with nuclear targets, in order to overcome these issues [13].

The region of interest with respect to this excess of scattering events is depicted in Figure 9 [14]. The point of cross-over between the QE and Inelastic interaction cross sections alone dips significantly, whereas the data indicates that the dip should not be quite as drastic. When adding in the MEC contribution and calculating the total cross section, this dip region increases to fit more closely with the data.

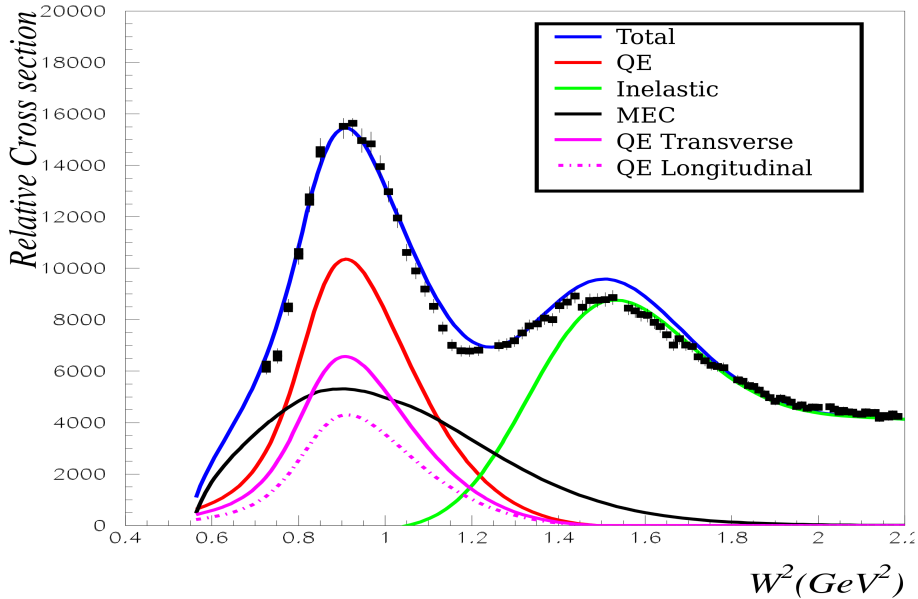


Figure 9: The contribution of various interactions to cross section predictions, it is only with the inclusion of MEC that the total cross section comes close to resembling that of data

Another indication that MEC is the cause of the observed excess is shown in Figure 10 [15]. In this diagram, various theoretical models are shown along with the data obtained. Here, most of the models fit to one another, but their cross sections collectively reside much lower than appears in the data. The closest fitting model to this data is the Martini, LFG+2p2h+RPA model, where 2p2h is the MEC contribution. Though tuning the parameter M_A also improves the RFG fit.

It is therefore clear that constructing model configurations with the correct physical theory is extremely important, but tuning the parameters which make up the models is also a crucial component in building predictions.

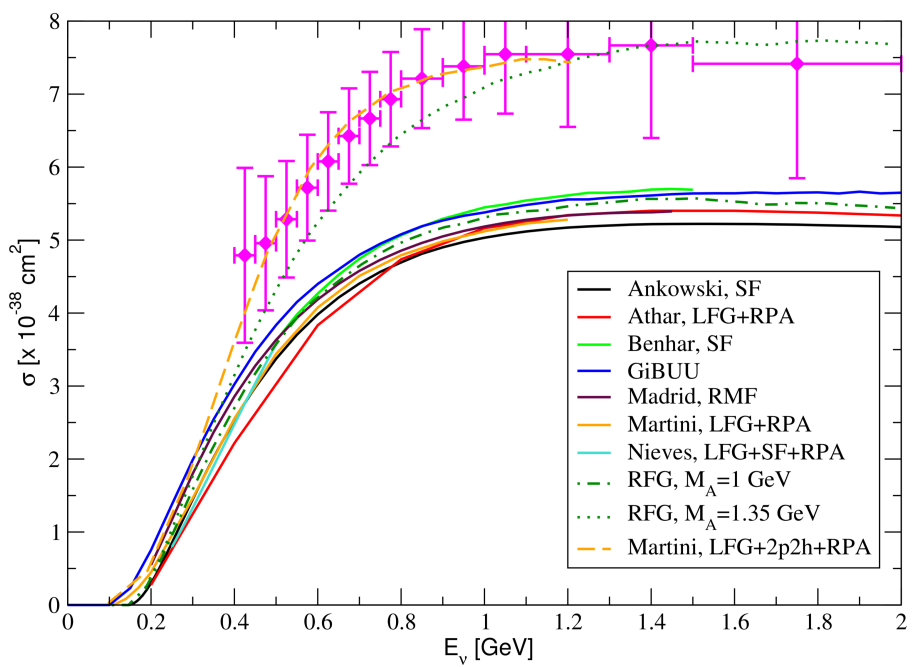


Figure 10: A collection of theoretical predictions made for the CCQE interaction compared with data, once again it is a model with the contribution of MEC which comes closest to correctly predicting the trend of the data, though tuning M_A improves the fit of the RFG model.

4. SBND Interaction Characterisation

To address these complications in practice, a preliminary exercise was carried out which aimed to characterise the expected initial and final state interactions for the observation of a CC0 π event in SBND. Alongside this, the potential backgrounds were also categorised in order to quantify their effect.

This exercise also contributed to the initial construction of an analysis framework which will eventually be expanded to incorporate fully reconstructed simulations and multiple final state topologies. In the first stage of this exercise however, a MC sample of neutrino events was generated using the G00_00b model configuration, described in Figure 15, and a manual amount of smearing was applied to them along with energy cuts and an application of pionic impurities in order to loosely represent reconstructed events in SBND whilst training the analysis framework.

4.1. Smearing

The Monte Carlo sample of SBND events was simulated using the Default+MEC GENIE model and the SBND flux, given in Figure 11. The quantities applied to the smearing, impurity additions and energy cuts are as follows ¹,

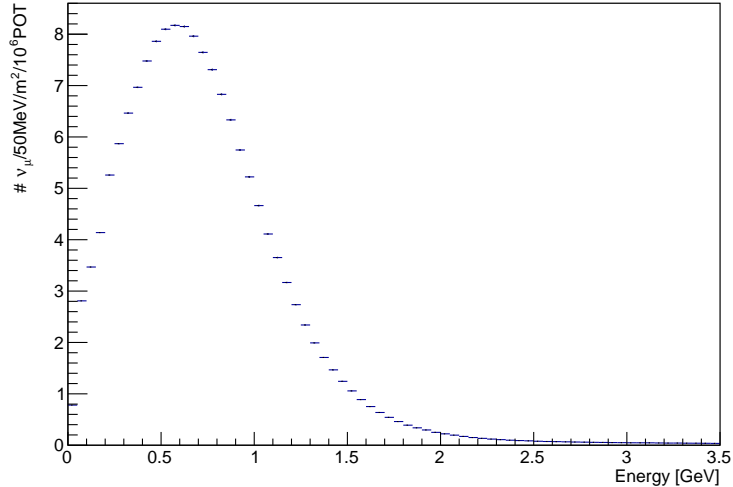


Figure 11: The flux of ν_μ at the short baseline near detector used to generate the neutrino events used throughout the following exercise

- Kinetic energy of the μ : 10%
- Opening angle of the μ : 5°
- μ kinetic energy threshold > 50 MeV

¹these quantities are in no way physically motivated. This entire analysis will eventually be implemented in a software framework which provides a dedicated reconstruction for liquid argon and so the smearing will not be a necessary step.

- π^\pm kinetic energy threshold > 50 MeV
- Proton kinetic energy threshold > 50 MeV
- NC $\pi^\pm \Leftrightarrow \mu$ mixup : 20% of π^\pm

To smear the angular quantities, a random point was chosen from a Gaussian distribution about the true angle with a standard deviation of 5° . Since the cosine of this angle was the variable of interest, if the smeared angle was below 0° the cosine of such a value would still be physically viable. However, a value of kinetic energy below 0 is not physically possible - since this implies the outgoing particles are travelling in the reverse direction to an interaction which occurred between a forward-going neutrino and a stationary nucleon. In this case, a lognormal distribution was used to randomly generate a kinetic energy with the true value as the mean, and a standard deviation of 10%.

The definition of a point on a lognormal distribution is given by equations (9), (10) and (11) and is shown entirely generally for 100,000 data points about a mean of 10 and a variance of 0.5 in Figure 12.

$$X = e^{(\mu+\sigma)} \quad (9)$$

$$\mu = \ln \left(\frac{m}{\sqrt{1 + \frac{v}{m^2}}} \right) \quad (10)$$

$$\sigma = \sqrt{\ln \left(1 + \frac{v}{m^2} \right)} \quad (11)$$

where m is the mean, v is the variance or standard deviation squared and X is the smeared data point.

In a CC0 π interaction, the potential backgrounds within the detector will contaminate the signal for various reasons, including:

- Low energy energy depositions of pions
- Mis-identification of pions
- ...

In this exercise, both the signal and background were split into potential contributing topologies in order to highlight the interaction characteristics within the detector and identify the channels which will be of interest in SBND.

4.2. Pre-FSI categorisation

Using MC information, it is possible to characterise the signal based on the true, interaction-level event topology. Reconstruction within a detector would not allow for this, but studying these distributions gives an idea of how frequently pions get absorbed and other internucleon interactions take place.

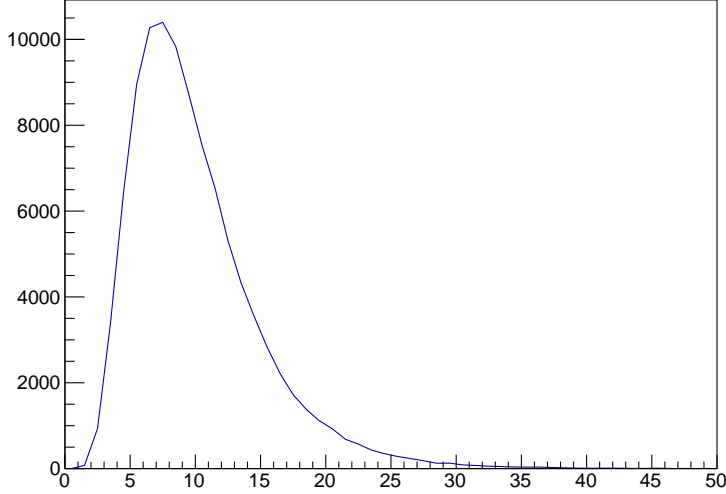


Figure 12: An entirely general lognormal distribution, this is used to calculate smeared kinetic energies because the points never go below 0. $T < 0$ MeV is an unphysical value in a detector which accepts a forward-going neutrino beam.

Figure 13 suggests that the dominant pre-FSI topology is a true CCQE event. It is also clear that multiple nucleon interactions, CCMEC, form a large portion of the CC0 π final state topology. Charged current resonant and other 1 π interactions contribute less, but are not negligible which suggests pions may frequently be emitted initially but never escape the nucleus.

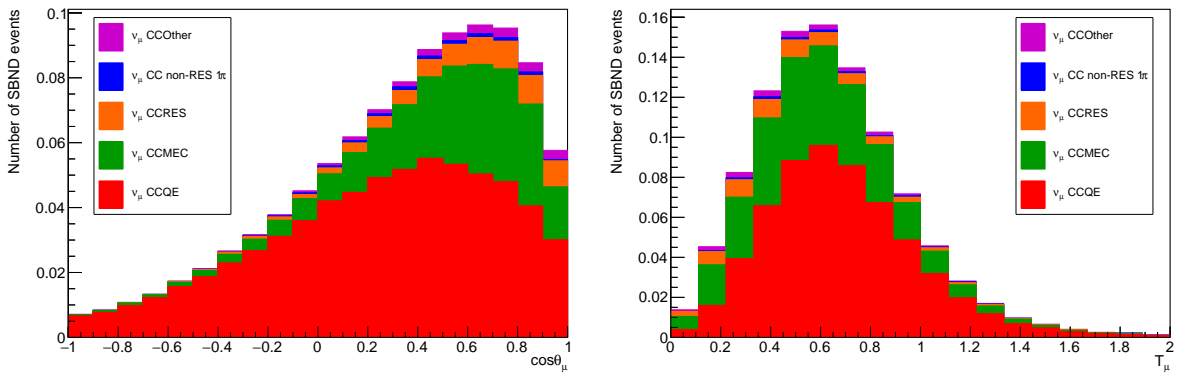


Figure 13: Area normalised muon kinetic energy and opening angle slices (left and right respectively) of the manually-reconstructed 2D distribution for CC0 π events. These slices have been split into various pre-final state interaction topologies in order to build a picture of the likely contributing factors to an observed CC0 π event: Charged current quasi-elastic (CCQE), charged current meson exchange current (CCMEC), charged current resonance (CCRES), charged current non-resonant single pion (CC non-RES 1 π) and other charged current interactions.

4.3. Post-FSI categorisation

The topologies chosen for study in the signal were based on the number of protons in the final state. Since the CC0 π interaction only involves a neutrino and one or more nucleons, determining the number of nucleons involved in the initial interaction is the main source of interest in the study of this topology.

The backgrounds were split into all other possible interactions which could take place in the detector, with 10% of charged current and 20% of neutral current interactions being accepted as backgrounds - these acceptances are chosen to be low due to the high resolving power of SBND, which should allow for good distinction between signal and background².

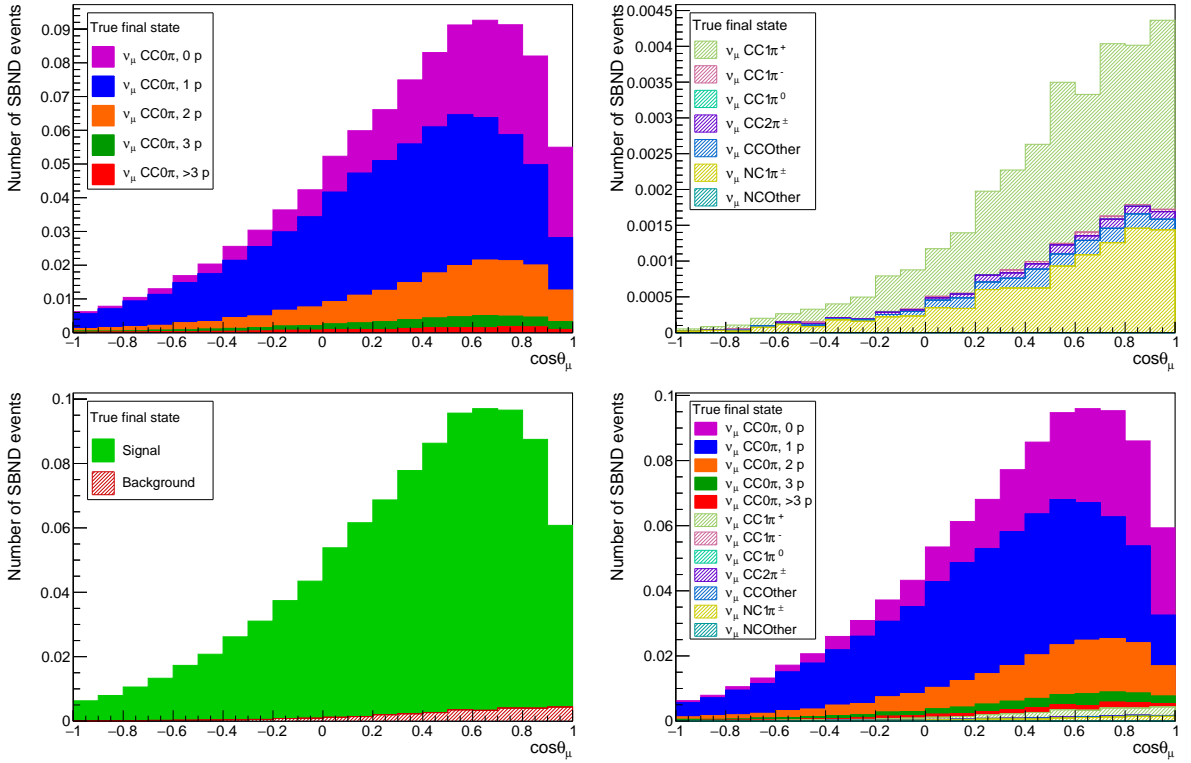


Figure 14: Top left: A breakdown of CC0 π signal events into topologies with different multiples of protons in the final state. Top right: Potential background event topologies. Bottom left: A comparison between signal and background shapes. Bottom right: All signal and background separated into topologies of interest.

The results shown in Figure 14 are the signal and backgrounds for CC0 π in SBND, characterised by splitting a slice of the 2D μ opening angle - kinetic energy distribution into different event topologies.

The signal is split into CC0 π, n protons. Where $0 < n$ in order to observe the contribution of the n particle n hole ($n p n h$) effect.

²Once again, the chosen percentage of backgrounds to include is not a physically motivated value, since this will be treated with much more care when external backgrounds such as cosmic and dirt events are included in the next stage of this analysis.

The backgrounds are split into charged current events with a single pion in the final state, charged current events with 2 charged pions in the final state, other charged current events, neutral current events with a single charged pion in the final state and other neutral current events. There should be no contribution from other neutral current events - this was included as a way of validating the method.

From these figures it is clear that the background topologies which will likely dominate in SBND for the CC 0π interaction are CC $1\pi^+$ and NC $1\pi^\pm$. The signal is dominated by events with low numbers of protons, which is to be expected when using 50 MeV energy thresholds on all particles. An event with more final state particles will likely give less energy to the individual particles which would then not be seen in the detector.

4.4. *Moving forwards*

Now that the signal and internal backgrounds events have been characterised, the analysis can be moved into the dedicated liquid argon software framework: LArSoft, which will incorporate the detector geometry, external background contributions, detector propagation effects and eventually full reconstruction. Before the full reconstruction is available however, more realistic smearing and impurity quantities will be determined in order to provide more accurate, manual reconstruction in the meantime.

An extention to this exercise would be to compare the smeared/reconstructed predictions with existing data to draw comparisons in a more realistic situation. The chosen experiment for this is MiniBooNE, which had the same baseline and energy range as SBND will have. For this reason, the kinematics studied were the same as that of MiniBooNE: muon kinetic energy as a function of the opening angle of the final state particles. An example comparison between MiniBooNE data and predictions made by GENIE is shown in Figure 17. The binning was also replicated in this exercise for the same reasons.

5. A Global Fit of CC0 π Data

5.1. GENIE and the comparisons

GENIE applies theoretical physics models, composed of both physical and unphysical parameters, to detector geometries and materials to build experiment-specific neutrino interaction predictions [3]. The collaboration is in the process of improving configurations of these models for the purpose of optimising the accuracy of the predictions.

An archive of experimental data is publicly available, and provides the key ingredient to this configuration update. Comparing the models with these data sets allows for a direct performance evaluation of the predictions, whilst fitting the models to the data enables the parameters to be tuned and consequently improve the prediction.

Summaries of the configuration of the GENIE models are as follows:

Name	Summary Description
G00_00a	GENIE v2 default model
G00_00b	GENIE v2 default + Empirical MEC model
G16_01a	Updated empirical model: An adiabatic change of the GENIE v2 default
G16_02a	A model anchored on best theory currently implemented in GENIE v3
G16_02b	As G16_02a, but replacing the hA with the hN FSI model

Figure 15: A brief overview the features which make up the individual model configurations in GENIE. These models will eventually all be tuned.

Details on the first model to be tuned (G16_01b) are as follows:

- Includes Empirical MEC
- CCQE process is Llewellyn-Smith Model
- Dipole Axial Form Factor - Depending on $M_A = 0.99$ GeV
- Nuclear model: Fermi Gas Model - Bodek, Ritchie

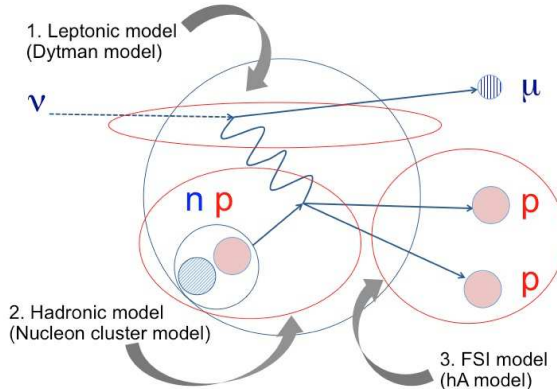


Figure 16: The models involved in the construction of the MEC model in neutrino event generation.

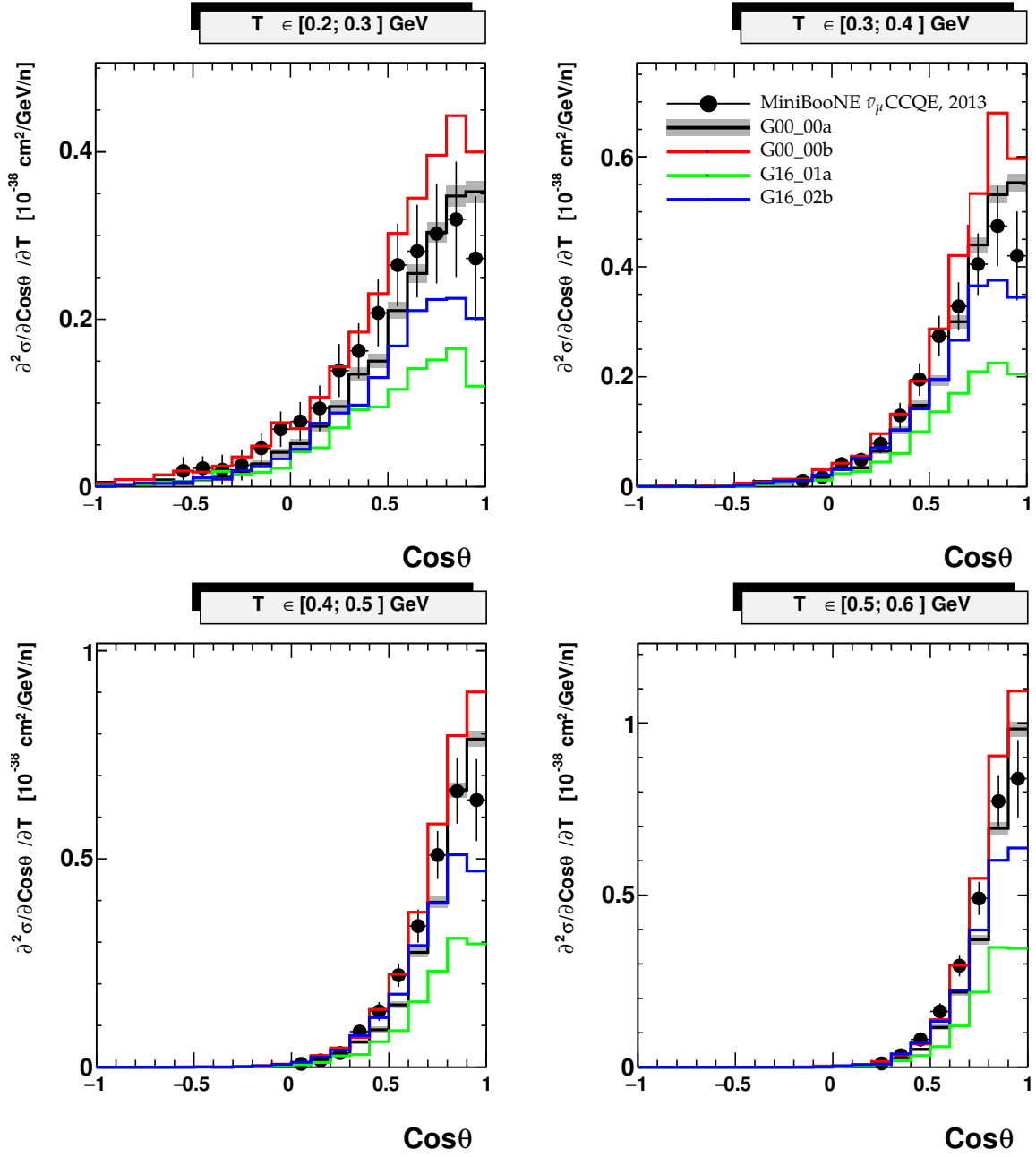


Figure 17: An example comparison between 4 GENIE models (described briefly in Figure 15) and MiniBooNE $\bar{\nu}_\mu$ CCQE data from 2013. The models fit the data with varying accuracies. It can be seen that even the closest fitting model is does not perfectly predict the trend seen in the data, therefore tuning is needed to fully optimise these fits.

This model takes the updated default GENIE model (G16_01a) and additionally addresses the abnormalities seen in recent experiments by incorporating the MEC interaction, described schematically in terms of the theoretical models involved in Figure 16 [13].

Datasets currently involved in the fit come from MiniBooNE, T2K and Minerva. An example of a comparison between the MiniBooNE $\bar{\nu}_\mu$ CCQE data set from 2013 and 4 different GENIE predictions is shown in Figure 17.

Although the G16_02b model is the most theoretically driven, it does not always provide the best fit to the data sets. For instance, in the MiniBooNE ν CCQE data from 2010, the G16_02b model fits better than both G00_00a and G00_00b, these fits are shown and quantified in Figure 19. However, in the MiniBooNE $\bar{\nu}$ CCQE data from 2013, Figure 18 shows that the G00_00b model had the best fit of the same three. Similarly in Figure 20 which is the comparison between the same models for the T2K ND280 ν CC0 π data from 2015, the G00_00a model fit best.

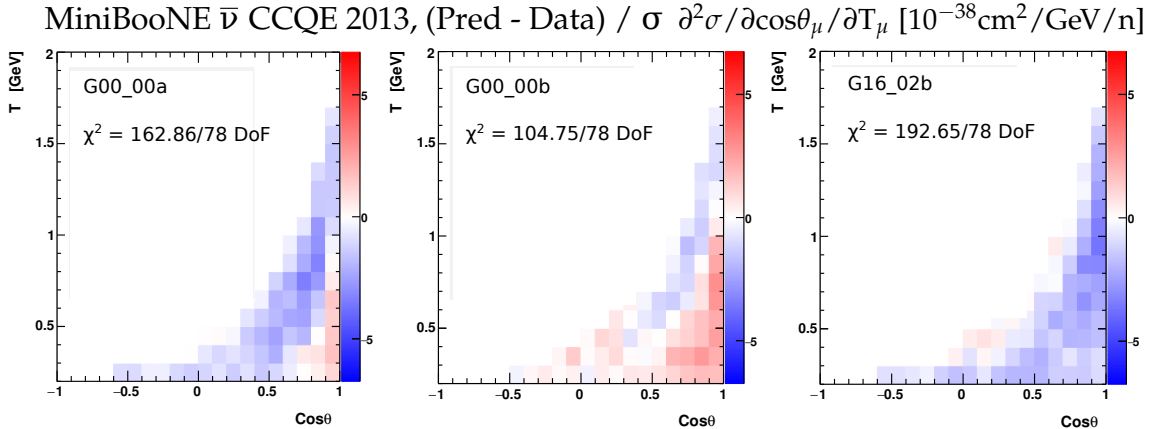


Figure 18: A comparison between the MiniBooNE $\bar{\nu}$ CCQE 2010 data set and 3 of the GENIE model configurations, left: G00_00a, middle: G00_00b, right: G16_02b. Taking the best fit to be the distribution with the lowest χ^2 / DoF , the G00_00b model predicts the dataset best.

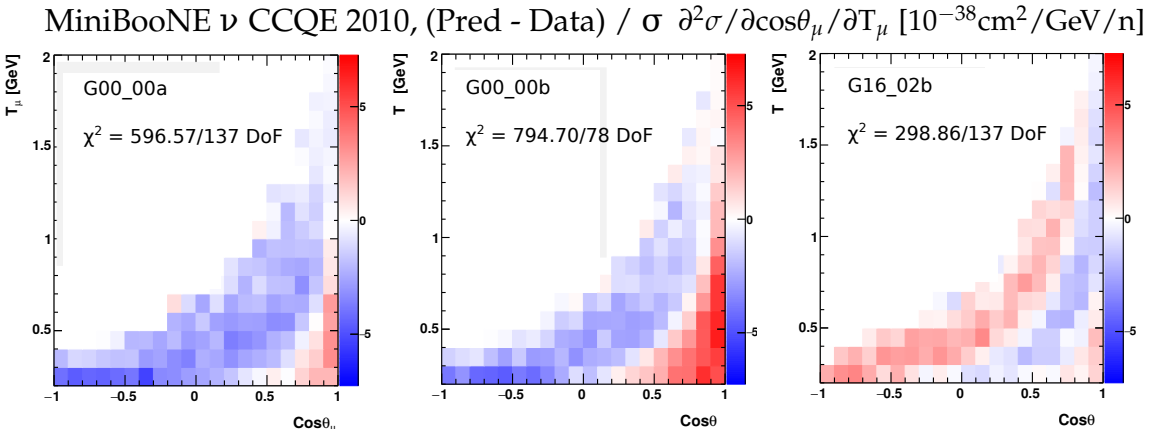


Figure 19: A comparison between the MiniBooNE ν CCQE 2013 data set and the same GENIE model configurations as in Figure 19. The same best fit definition means the G16_02b model predicts the dataset best.

Clearly, there are tensions between the datasets and no single theory best predicts all data. This tension will be a focal point when analysing the tuning results.

5.2. Professor

The Professor software framework parameterises the Monte Carlo event generator's response to parameter shifts on a bin-by-bin basis [4]. The tuning is done through fitting parameters within models to data and has the ability to incorporate multiple parameters within models as well as fitting together multiple data sets. Professor therefore provides the opportunity to perform global tunings of theoretical models based on the extensive archive of neutrino scattering data which is publically available.

The tuning is done in a subset of parameter space rather than on the full Monte Carlo, this space is defined by the x-axis in Figure 21 which is a schematic diagram of the fitting

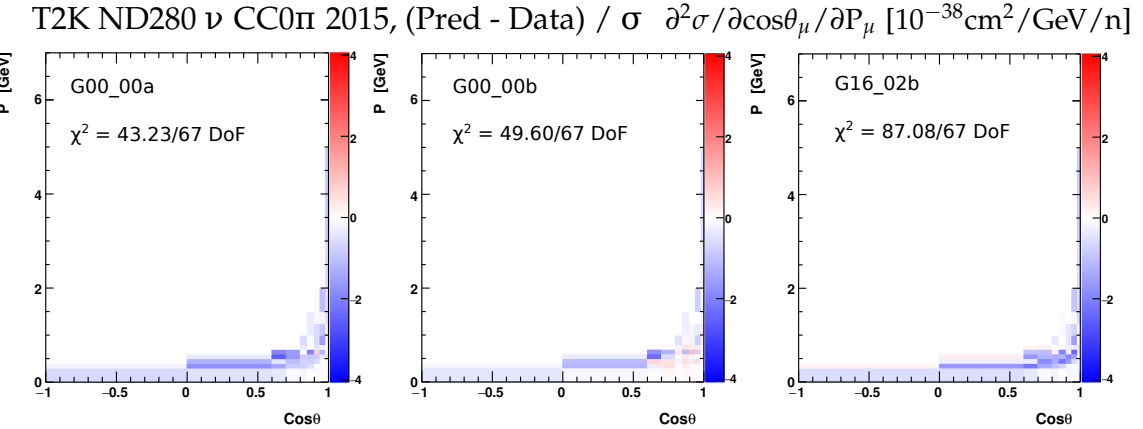


Figure 20: A comparison between the T2K ν CC0 π 2015 data set and the same GENIE model configurations as in Figures 19 and 18. The same best fit definition means the G00_00a model predicts the dataset best.

process. Only parameterising a sample of the Monte Carlo drastically reduces the computational expense of the process. The tuning is performed on multiple parameters in one go, and the nominal value for each is calculated using a χ^2 minimisation [4].

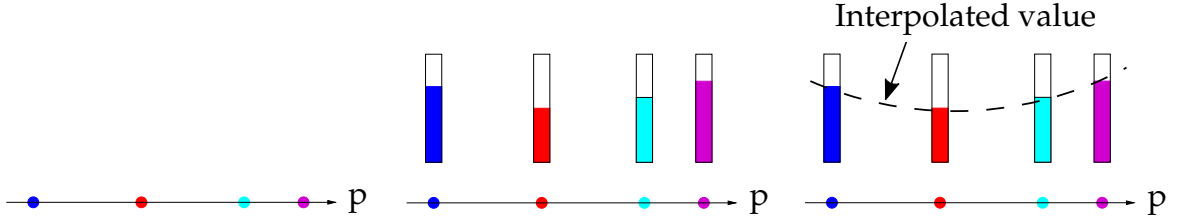


Figure 21: A schematic of the Professor tuning method. Left: the parameter space is selected. Middle: The behaviour of each parameter in an individual bin is observed. Right: A parameter-dependent interpolation is constructed $I(p)$ from the whole parameter space. The process is repeated for every bin.

5.3. Results

To date, the fit has been performed on 6 parameters within the G16_01b model, the results of which are given in Figure 22 alongside the nominal - most physical - value for each.

Parameter	Neutrino fit	Anti-neutrino fit	Global fit	Nominal value
M_A (GeV/c 2)	1.17 ± 0.02	1.26 ± 0.03	1.21 ± 0.02	0.99
QEL-CC-XSecScale	0.93 ± 0.01	0.97 ± 0.02	0.95 ± 0.02	1
RES-CC-XSecScale	0.86 ± 0.05	0.98 ± 0.09	1.02 ± 0.05	1
MEC-FracCCQE	0.85 ± 0.03	0.7 ± 0.1	0.53 ± 0.08	0.45
FSI-PionMFP-Scale	0.87 ± 0.02	1.39 ± 0.03	0.75 ± 0.04	1
FSI-PionAbs-Scale	1.51 ± 0.03	0.7 ± 0.1	0.87 ± 0.07	1

Figure 22: Parameter fit results.

Towards the global fit, the G16_01b model was also tuned separately to 5 sets of data: MiniBooNE CCQE ν_μ , MiniBooNE CCQE $\bar{\nu}_\mu$, Minerva CCQE ν_μ , Mineva CCQE $\bar{\nu}_\mu$ and T2K CC 0π . The results of the individual and global fits are given in Figure 23

Fit Results	Neutrino fit	Anti-neutrino fit	Global fit	Nominal Values
Miniboone $\nu_\mu \chi^2$	152 / 137	171 / 137	138 / 137	441 / 137
MiniBooNE $\bar{\nu}_\mu \chi^2$	60 / 78	32.4 / 78	36.2 / 78	50.4 / 78
T2K χ^2	237 / 67	276 / 67	252 / 67	135 / 67
MINERvA $\nu_\mu \chi^2$	6.11 / 8	8.07 / 8	7.79 / 8	17.5 / 8
MINERvA $\bar{\nu}_\mu \chi^2$	8.19 / 8	11.5 / 8	5.7 / 8	6.23 / 8
Global dataset χ^2	463 / 292	499 / 292	440 / 292	650 / 298

Figure 23: Experiment fit results.

Graphical slices of the experimental results for MiniBooNE ν_μ , Minerva ν_μ and T2K are shown in Figure 24 in order to visually demonstrate the comparison between the model before and after tuning on each data set.

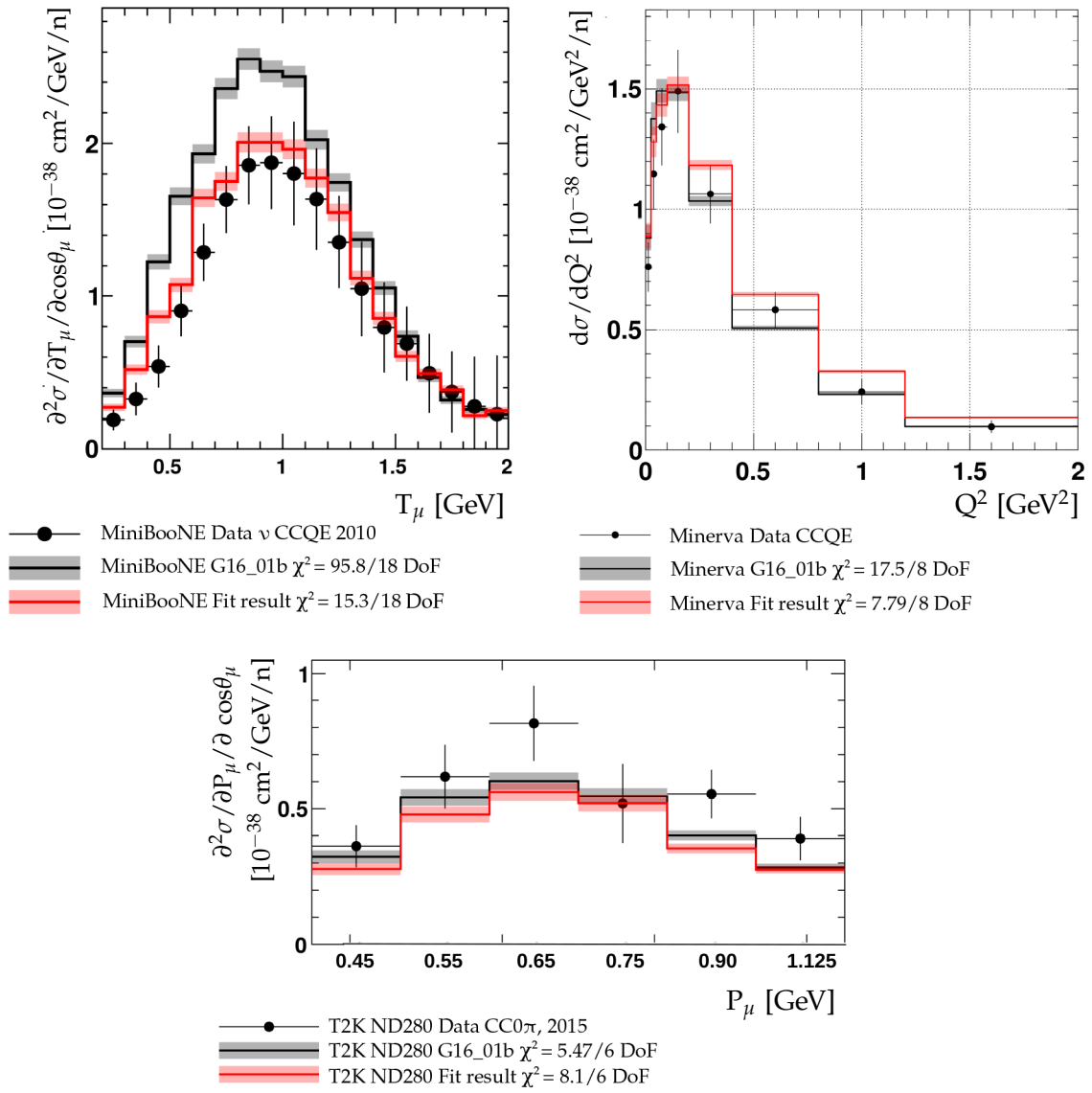


Figure 24: Global fit results.

6. Theory and Recent Measurements of CC 0π Cross-Section

6.1. *Cross-sections*

- Theory
 - Simulation
 - GENIE
 - Historical
 - Current knowledge
 - Needs for future
 - LArTPCs
 - Statistics
- Inc. equations

6.2. *Method*

6.3. *Unfolding*

6.4. *Results*

Plots and cross-section values

7. Prospects for a CC0 π Measurement at SBND and Sensitivity Estimates

7.1. *Discussion*

7.2. *SBND sensitivity*

7.3. *Conclusion and Future*

References

- [1] Kevin Scott McFarland. Neutrino Interactions. pages 65–90, 2008.
- [2] Y. Fukuda et al. Evidence for oscillation of atmospheric neutrinos. *Phys. Rev. Lett.*, 81:1562–1567, 1998.
- [3] Costas Andreopoulos, Christopher Barry, Steve Dytman, Hugh Gallagher, Tomasz Golan, Robert Hatcher, Gabriel Perdue, and Julia Yarba. The GENIE Neutrino Monte Carlo Generator: Physics and User Manual. 2015.
- [4] Andy Buckley, Hendrik Hoeth, Heiko Lacker, Holger Schulz, and Jan Eike von Seggern. Systematic event generator tuning for the LHC. *Eur. Phys. J.*, C65:331–357, 2010.
- [5] J. A. Formaggio and G. P. Zeller. From eV to EeV: Neutrino Cross Sections Across Energy Scales. *Rev. Mod. Phys.*, 84:1307–1341, 2012.
- [6] M. Antonello et al. A Proposal for a Three Detector Short-Baseline Neutrino Oscillation Program in the Fermilab Booster Neutrino Beam. 2015.
- [7] A. A. Aguilar-Arevalo et al. Unexplained Excess of Electron-Like Events From a 1-GeV Neutrino Beam. *Phys. Rev. Lett.*, 102:101802, 2009.
- [8] Dinko Pocanic, Emil Frlez, and Andries van der Schaaf. Experimental study of rare charged pion decays. *J. Phys.*, G41:114002, 2014.
- [9] B. Baller et al. Liquid Argon Time Projection Chamber Research and Development in the United States. *JINST*, 9:T05005, 2014.
- [10] C. Patrick. Microboone sees first accelerator-born neutrinos. http://www.fnal.gov/pub/today/archive/archive_2015/today15-11-02.html, 02-11-2015. Cited on 27-04-2017.
- [11] R. Acciarri et al. Design and Construction of the MicroBooNE Detector. *JINST*, 12(02):P02017, 2017.
- [12] Teppei Katori and Marco Martini. Neutrino-Nucleus Cross Sections for Oscillation Experiments. 2016.
- [13] Teppei Katori. Meson Exchange Current (MEC) Models in Neutrino Interaction Generators. *AIP Conf. Proc.*, 1663:030001, 2015.
- [14] A. Bodek, H. S. Budd, and M. E. Christy. Neutrino Quasielastic Scattering on Nuclear Targets: Parametrizing Transverse Enhancement (Meson Exchange Currents). *Eur. Phys. J.*, C71:1726, 2011.
- [15] Luis Alvarez-Ruso. Neutrino interactions: challenges in the current theoretical picture. *Nucl. Phys. Proc. Suppl.*, 229-232:167–173, 2012.